Quasi-coherent noise-like pulses in a mode-locked fiber laser with 3D rotatable polarization beam splitter

RENLAI ZHOU,[1,2,5] QIAN LI,[2*] H. Y. FU,[3] AND K. NAKKEERAN[4]

[1]*Naval University of Engineering, Wuhan, 430033, China*
[2]*School of Electronic and Computer Engineering, Peking University, Shenzhen, 518055, China*
[3]*Tsinghua-Berkeley Shenzhen Institute (TBSI), Tsinghua University, Shenzhen, 518055, China*
[4]*School of Engineering, Fraser Noble Building, University of Aberdeen, Aberdeen AB24 3UE, United Kingdom*
[5] *zrlhit@126.com*
**Corresponding author: liqian@pkusz.edu.cn*

Received XX Month XXXX; revised XX Month, XXXX; accepted XX Month XXXX; posted XX Month XXXX (Doc. ID XXXXX); published XX Month XXXX

For the first-time, we experimentally observed a novel type quasi-coherent noise-like pulses in a simplified nonlinear polarization evolution mode-locking fiber laser when appropriate polarization was maintained for the lasing light through a three-dimensionally rotatable polarization beam splitter inside the cavity. The degree of first-order coherence was evaluated after an interferogram measurement. Evolution of the measured shot-to-shot spectrum revealed that the noise-like pulses possess quasi-coherence. Self-started ultrafast soliton pulses switching to quasi-coherent noise-like pulses at higher pump power levels were due to the preservation of the soliton features, mainly the Kelly sidebands in the spectrum. Quasi-coherent noise-like pulses with average power of 56.58 mW and 10.4% slope efficiency were achieved with single pulse energy of 3.22 nJ.

http://dx.doi.org/10.1364/OL.99.099999

Special mode-locked pulses called the noise-like pulses (NLP) was first demonstrated in an erbium-doped fiber (EDF) laser by Horowitz et al., [1] and it attracted interests in both research and applications owing to their extraordinary features. Compared to the soliton pulses (SP), the NLP could possess high energy which could reach up to a level of μJ, and wider pulse duration which could reach hundreds of nanoseconds. NLP with various pulse-shapes were also demonstrated in fiber lasers [2], that includes Gaussian-, rectangular-, trapezoidal-shaped pulses and bunched-pulses. Due to these versatile properties, NLP found potential applications in the fields of micromachining [3], supercontinuum generation [4], and low spectral coherence interferometry [5].

Generally, NLP have a compact wave packet profile that contains a bunch of ultrashort pulses with random intensity and duration in the time domain, and a smooth and broad spectrum in the frequency domain. Due to the random tiny pulses within its wave packet, there was no measurable phase coherence in the NLP that were generated in different configurations of mode-locked fiber lasers that were reported so far in the literature. Runge et al., [6] measured the pulse-to-pulse fluctuations in the NLP by monitoring the single-shot spectrum, and found that the fringe visibility showed no phase coherence in the NLP regime. However, Kwon et al., [7] observed a weak spectral interference pattern between two consecutive NLP, and reported the feasibility of partially-coherent NLP. Same research group, theoretically studied the shot-to-shot coherence of laser pulses in different quasi-mode-locking regimes, and reported that both the laser cavity configuration and the net-cavity dispersion play critical roles in the generation of partially-coherent NLP [8]. To our knowledge, until now, no experimental demonstration of the generation of NLP with high amount of partial phase coherence (quasi-coherence) was observed.

In this work, we report the first-time experimental observation of a novel quasi-coherent NLP with Kelly sidebands spectrum in a simplified mode-locked fiber laser setup with a 3D rotatable polarization beam splitter (PBS) within its cavity. The output characteristics of the NLP were investigated for different pump powers, which assisted in the understanding of the dynamics of the proposed mode-locked fiber laser that can be switched from SP regime to stable quasi-coherent NLP regime. The measured interferogram indicated that the first-order coherence of the generated NLP was greatly improved due to the preservation of the soliton features, mainly the Kelly sidebands in its spectrum.

Different from other nonlinear polarization evolution (NPE) mode-locked lasers, the bulk optical devices like half-wave and quarter-wave plates were not included. Instead, a 3D rotatable PBS was deployed on a horizontal surface within the cavity. Schematic of the fiber laser setup is shown in Fig. 1. The polarization states of the optical signal lasing in the laser cavity could be fine-tuned by three-dimensional maneuvering of the PBS position. The gain was provided by a 1 m long EDF (EDFL-980-HP, Nufern), which was

pumped by a 976 nm laser diode (LD) through a 980/1550 nm wavelength-division multiplexer (WDM). An in-line polarization controller (PC) was included to enhance the mode-locking. Two fiber collimators were used for positioning and coupling of the light signal, with a coupling efficiency of about 75%. A polarization-insensitive isolator (PI-ISO) was added for unidirectional light propagation in the laser cavity. Total cavity length was ~11.64 m with a net-cavity dispersion of –0.338 ps^2, indicating that the mode-locking operated in the anomalous dispersion regime. Output spectrum and pulse-train were monitored by an OSA (AQ6370D, Yokogawa, resolution 0.02 nm) and a real-time 59 GHz bandwidth oscilloscope (DPO-75902SX, Tektronix) connected via an ultrafast response InGaAs photodiode detector (UPD-15-IR2-FC, >25 GHz bandwidth). The RF of laser operation was monitored by a signal analyzer (N9030B, Agilent) which has a bandwidth of 3 Hz – 50 GHz.

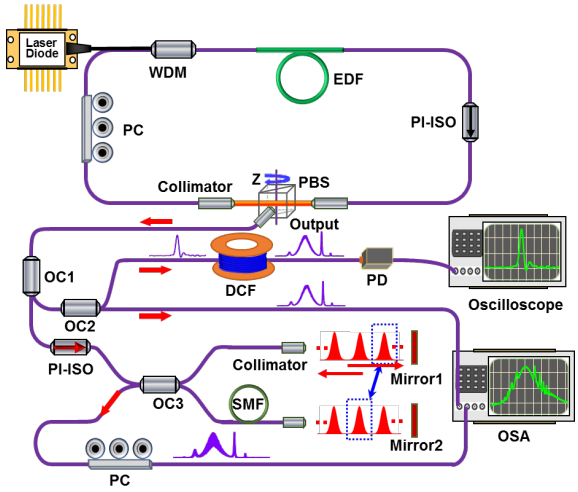

Fig. 1. Schematic of a simplified NPE mode-locked fiber laser. OSA - optical spectrum analyzer; OC1, OC2, OC3 - 3-dB optical couplers.

In this proposed NPE mode-locked fiber laser, the polarization states of the transmitted beam from the PBS were regulated by maneuvering the PBS along *z* axis [9]. The SP were generated in the fiber laser, when the PBS was steered about 4.5 degrees clockwise. Mode-locked multi-pulse state SP was self-stared when the pump power was raised to 135 mW. Then, the pump power was lowered to 100 mW for the cavity to mode-lock single stable SP. When the pump power was reduced to 70 mW, the cavity went out of mode-locking. Measured output spectra are depicted in Fig. 2(a), where the red and blue curves, represent the continuous-wave (CW) signal and SP. On the SP spectrum, Kelly sidebands were observed and the 3-dB spectral bandwidth was measured as 6.84 nm. The monitored pulse-train and RF spectrum (resolution bandwidth 1 Hz) are shown in Figs. 2(b) and 2(c). Measured SP period was ~56.95 ns which corresponds to the cavity roundtrip time. The pulse repetition rate was 17.55882 MHz which coincides to the fundamental repetition rate. Signal-to-noise ratio (SNR) measured above 90 dB indicated a highly stable SP operation in this cavity. A wideband RF spectrum up to 1.5 GHz presented in Fig. 2(c) inset disclosed that the SP operation was very stable. The corresponding intensity autocorrelation (AC) trace is shown in Fig. 2(d). The full width at half maximum (FWHM) pulse duration was ~460.1 fs, that was calculated through a sech^2 profile fit for the measured pulse. The time-bandwidth product calculated as 0.4 was nearly the transform-limited value 0.315 of a chirp-free sech^2-shaped pulse.

When the pump power was further increased to 225 mW, the soliton state switched to a different stable pulsating mode-locked state in the cavity. Measured spectral and temporal characteristics of the new state are depicted in Figs. 2(e)-2(h). In the frequency domain, compared to the SP state the new state possessed a broadband spectrum and increased intensity, as shown in Fig. 2(e) and more interestingly, a series of spikes were observed. The spectral spikes were related to the Kelly sidebands. The phase-matching condition of the Kelly sidebands can be calculated as $2\pi N = D/2\times(\omega^2+1/\tau^2)$, where N is the order of the sidebands with an angular frequency offset of ω from the central frequency ω_0, 1.763τ is the FWHM of the SP duration, and $D = 4\pi/(\omega_2^2-\omega_1^2)$ is the net-dispersion of the cavity, with $\omega_{1,2}$ as the frequency offset of the two adjacent spikes from the central frequency [10]. Measured central frequency ω_0 = ~836.911 THz, and the computed right and left frequency locations of the spikes shown in Fig. 2(e) were R_1 = 0.936, R_2 = 1.936, R_3 = 2.953, R_4 = 4.04, R_5 =5.049, R_6 = 6.061, L_1 = 0.966, L_2 = 2.044, L_3 =3.022, L_4 = 4.078. As

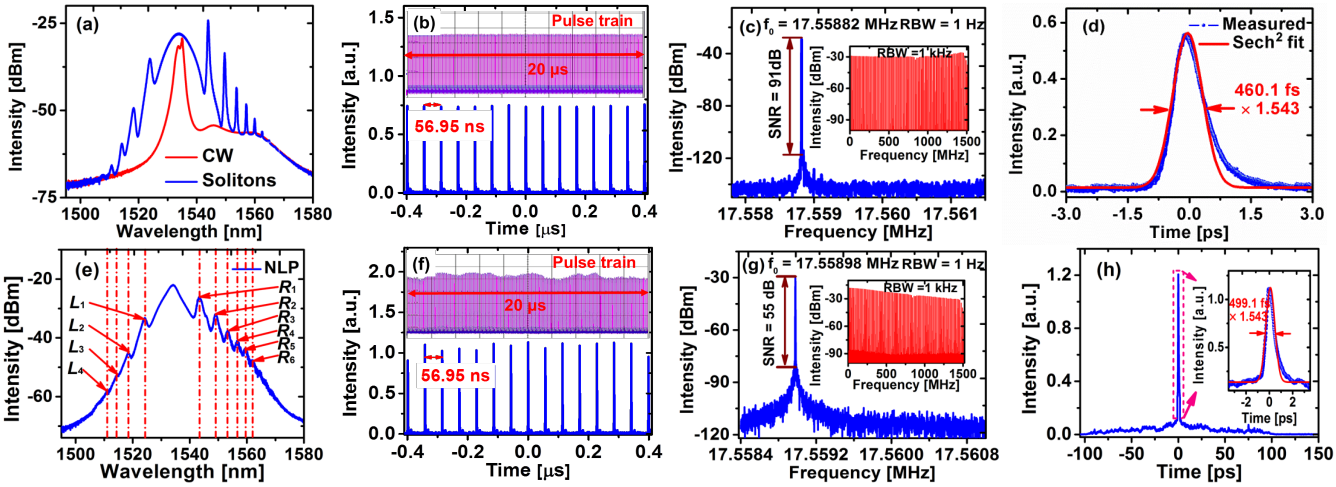

Fig. 2. Output features of SP (a-d) and NLP (e-h): (a), (e) output spectrum; (b), (f) pulse-train; (c), (g) RF spectrum; (d), (h) intensity AC trace.

expected, the calculated frequency locations of the spikes coincided with the OSA recorded spectrum, revealing that the spikes on the spectrum belonged to Kelly sidebands that met the phase matching conditions. Measured output pulse-train is shown in Fig. 2(f), in which the adjacent pulses temporal separation was same as that of the SP, but intensity fluctuations were observed in the profile of the pulse-train, which implied that the single pulse energy of this state was not steady. Pulse repetition rate was 17.55898 MHz, as presented in Fig. 2(g), and it was about 160 Hz frequency shifted compared with that of the SP. SNR measured as 55-dB indicated that this novel mode-locking can operate reliably, but the stability was less than the soliton state. Finer details of the laser pulse are presented in Fig. 2(h). A double-scale structure with a narrow pulse peak (~499.1 fs) riding on top of a broad pedestal was observed, which is a typical feature of NLP. Hence this mode-locked operation is classified as the NLP regime. However, different from the previous reported results [2, 6-8], the intensity of the measured narrow pulse peak was much higher than its pedestal, and the intensity ratio between the narrow pulse peak and the pedestal was about 14. This feature implies that the soliton characteristics were preserved in the observed NLP that played a dominant role in the dynamics of this state. Mainly, the Kelly sidebands occurred as spikes on the NLP spectrum confirmed the soliton feature in this state, which was first time observed in NLP generated in any mode-locked fiber lasers reported so far.

To investigate other characteristics of the SP and NLP lasing in the cavity at different pump power levels, average laser output powers were measured. As depicted in Fig. 3(a), the entire mode-locking operation can be divided into three regimes: SP regime, unstable regime and NLP regime. In the SP regime with the self-start threshold pump power of 135 mW, the mode-locked pulse(s) average power linearly increased with a slope efficiency of 11.67% for increasing pump power. The maximum output power reached was 19.45 mW at a pump power of 180 mW. Stable single SP lased for the pump power range of 70–100 mW and between 100–180 mW; stable multi-pulse SP lased. In the pump power range of 180–225 mW, the switching between SP and NLP regimes happened randomly, and hence termed as unstable regime. Stable NLP lasing started from a pump power amount of 225 mW. In the NLP regime, the output power grew linearly with a slope efficiency of 10.4%, and an average power of 56.58 mW was achieved at a maximum achievable pump power of 540 mW of the source used. Within the saturation limit of the available pump source, the measured pulse energy of the NLP at fundamental repetition rate, linearly increased from 1.36–3.22 nJ. Higher energy NLP beyond this range maybe feasible in the proposed fiber laser with high powered pump source. Various regimes output signal spectra at different pump powers are presented in Fig. 3(b). Measured spectral profiles of SP and NLP regimes were different. Their respective spectral intensity value increased with increasing pump power,

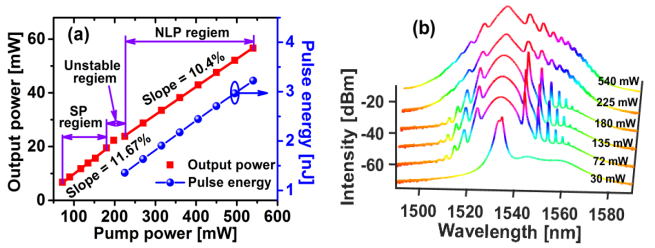

Fig. 3. Pump power VS average output power (a) and spectra (b).

without causing any changes in their spectral profile or bandwidth.

In a mode-locking soliton spectrum, Kelly-sidebands are formed because of the interference superposition between the soliton pulses and dispersive waves, when their relative phase changes by an integer multiple of 2π per cavity roundtrip time. Thus, the presence of Kelly-sidebands is a strong evidence for the coherence of the mode-locked pulses. In order to evaluate the first-order phase coherence of the cavity signal, a fiber Michelson interferometer was constructed to measure the cross-coherence of adjacent pulses, as shown in Fig. 1. Using single-mode fiber, one arm of the interferometer was constructed longer than the other by exactly one half of the cavity roundtrip time. The signals in the respective arms were collimated, and 100% reflected by two separate gold-coated mirrors. For the finer adjustments of the temporal overlap between the two signals at the interferometer output, one of the mirrors was mounted on a precise translation stage. An in-line PC was used to maintain same polarization states between the interfering signals from both arms. The spectral interference fringes were measured through OSA, that recorded every sweep with an ensemble average of >3×10^6 interference events from which the first-order coherence $g_{12}^{(1)}$ between adjacent pulses was calculated with [11]:

$$\left|g_{12}^{(1)}(\lambda)\right| = \frac{[I_1(\lambda)+I_2(\lambda)]V(\lambda)}{2[I_1(\lambda)I_2(\lambda)]^{1/2}} \quad \textbf{(1)}$$

where $I_{1,2}(\lambda)$ represent the measured spectral intensities from two arms. The fringe visibility $V(\lambda)$ is computed using the measured maximum and minimum fringe intensities as $V(\lambda) = [I_{max}(\lambda) - I_{min}(\lambda)]/[I_{max}(\lambda) + I_{min}(\lambda)]$. Before the spectral interference measurements were made, precise adjustments were carried out for the temporal overlapping between adjacent pulses to select adequate fringe spacing. Figure 4(a) depicts the spectral interference pattern and first-order coherence of the SP. Nearly ~100% spectral modulation depth suggested high degree of phase coherence in SP regime, and the calculated first-order coherence $g_{12}^{(1)}$ is ~0.945 over the major portion of the spectrum. With increase in pump power; switching happened from SP to NLP, for the spectral interference pattern and first-order coherence to be transformed as shown in Fig. 4(b). Contrary to the earlier report [9], the interference pattern was still present in almost the entire spectrum of the NLP. But the modulation depth was less than that in SP regime, indicating the degradation of pulse-to-pulse phase coherence in the NLP regime. Noticeable fluctuations were observed in the first-order coherence, and high coherence values

were found at the locations where Kelly-sidebands were present. The zoomed-in snapshots of spectral regions at 1528–1533 nm and 1548–1553 nm are shown in Figs. 4(c) and 4(d), and the corresponding average first-order coherence values were calculated as ~0.462 and ~0.652, respectively. Though the phase coherence of NLP underwent some degradation compared to the SP, the first-order coherence value throughout the spectrum was found to be above ~0.408. The presence of Kelly sidebands acknowledges the coherence of the mode-locked signal and the strength of the first-order coherence determines the quality of the coherence. Even though, shot-to-shot coherence properties in quasi-mode-locked regime were already theoretically investigated [8], spectra obtained through simulations were different from the measured NLP spectra. Due to short cavity length of around 12 m,

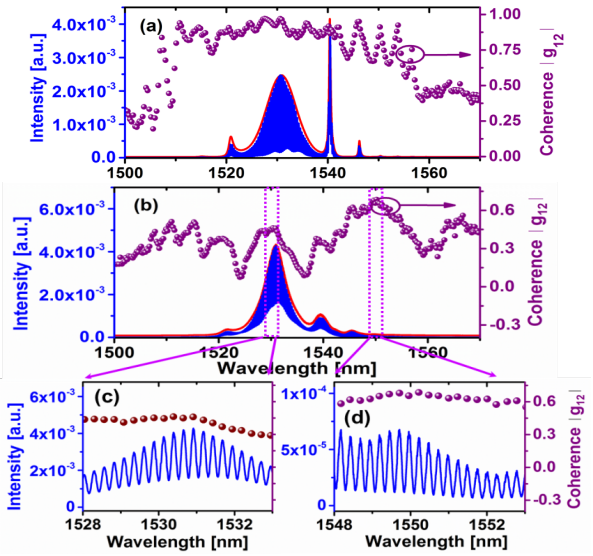

Fig. 4. Measured spectral interference pattern and calculated first-order coherence: (a) SP regime; (b) NLP regime.

the dynamics of collapse of solitons and interactions between sub-pulses within a packet were evaded [12, 13]. This resulted in the lasing of relatively more regular soliton pulses even during the NLP regime, which maintained the coherence of the NLP. Besides every pulse of the NLP, weak sub-pulse was observed. Peak power ratio of ~0.05 was maintained between sub-pulse to main-pulse for various pump powers. These sub-pulses were the coherent part (SP) of the NLP that did not collapse or completely merge with the main pulse and provided the quasi-coherency for the NLP. The main pulse and the sub pulse were coupled and simultaneously mode-locked in the fiber laser cavity at the same wavelength.

A single-shot spectrum measurement was carried out through a time-stretch dispersive Fourier transform technique (TS-DFT) [14, 15] in a 1 km long dispersion-compensating fiber (DCF) with a dispersion of ~178.4 ps^2, corresponding to a spectral resolution of ~0.11 nm. The real-time spectral profiles of 1000 consecutive roundtrips were obtained in a single-shot capture, and the reconstructed sequence of the spectral evolution is shown in Fig. 5. It is evident that the soliton single-shot spectrum almost replicated the OSA measured spectrum shown in Fig. 5(a). The single-shot soliton spectrum was indistinguishable from each another, resulting in a stable output spectrum with good phase correlation. In contrast to the almost invariable soliton spectrum, the NLP spectrum exhibit fluctuations [Fig. 5(b)]. Despite good profile exhibited in each single-shot spectrum, the spectral intensity distribution was quite different from the earlier reported incoherent NLP [2, 6]. Most of the NLP spectral energy was confined in and around the central wavelength with no incoherent sidebands in the shot-to-shot spectra measured by TS-DFT [16], which is a familiar characteristic of soliton spectrum. This is another evidence apart from the appearance of Kelly sidebands (spikes) on the NLP spectrum to confirm that the NLP possessed more of SP characteristics including the phase coherence.

To conclude, in a simplified NPE fiber laser with 3D rotatable PBS, we experimentally demonstrated the mode-locking of quasi-coherent NLP with Kelly sidebands in its spectrum. By adjusting the pump power, the self-started pulses can switch from soliton state to NLP state that maintained most features of solitons. To our

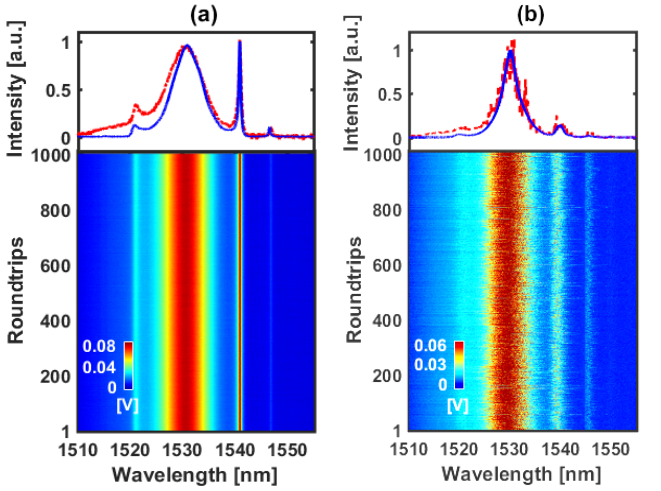

Fig. 5. Single-shot spectral evolution for (a) SP and (b) NLP regime. (Top) The blue solid curve shows the OSA spectrum and the red dashed curve shows an arbitrarily picked single spectrum.

knowledge, this was the first-time experimental observation of high-energy noise-like ultrafast laser pulses with a high amount of coherence due to preservation of soliton properties. We believe that the reported results introduced a novel nonlinear operation regime of mode-locked ultrafast fiber lasers that can provide useful insights into the quasi-coherent NLP ultrafast fiber laser designs and applications.

Funding. National Science Foundation of China (NSFC) (61805281); Natural Science Foundation of Guangdong Province, China (2019A1515010732).

Disclosures. The authors declare no conflicts of interest.

REFERENCES

1. M. Horowitz, Y. Barad, and Y. Silberberg, Opt. Lett., **22**, 781 (1997).
2. Y. Jeong, L. A. V. Zuniga, S. Lee, and Y. Kwon, Opt. Fiber Technol., **20**, 575 (2014).
3. K. Özgören, B. Öktem, S. Yilmaz, F. Ö. Ilday, and K. Eken, Opt. Express, **19**, 17647 (2011).
4. A. Zaytsev, C. Lin, Y. You, C. Chung, C. Wang, and C. Pan, Opt. Express **21**, 16056 (2013).
5. S. Keren and M. Horowitz, Opt. Lett. **26**, 328 (2001).
6. A. F. J. Runge, C. Aguergaray, N. G. R. Broderick, and M. Erkintalo, Opt. Lett., **28**, 4327 (2013).

7. Y. Jeong, L. Alonso, V. Zuniga, S. Lee, and Y. Kwon, Opto-Electronics and Communications Conference (OECC), 1 (2015).
8. Y. Kwon, L. A. Vazquez-Zuniga, S. Lee, H. Kim, and Y. Jeong, Opt. Express **25**, 4456 (2017).
9. J. Shang, X. Lu, T. Jiang, Y. Lu, and S. Yu, Opt. Lett. **43**, 3301 (2018).
10. L. E. Nelson, D. J. Jones, K. Tamura, H. A. Haus, E. P. Ippen, Appl. Phys. B **65**, 277 (1997)
11. J. M. Dudley, S. Coen, Opt. Lett. **27**, 1180 (2002).
12. A. I. Chernykh, and S. K. Turitsyn, Opt. Lett. **20**, 398 (1995).
13. D. Tang, L. Zhao, and B. Zhao, Opt. Express **13**, 2289 (2005).
14. Y. C. Tong, L. Y. Chan, and H. K. Tsang, Electron. Lett. **33**, 11 (1997).
15. K. Goda, and B. Jalali, Nature Photon. **7**, 102 (2012).
16. M. Liu, H. Chen, A. Luo, G. Zhou, Z. Luo, and W. Xu, IEEE J. Sel. Top. Quantum Electron. **24**, 1100606 (2017).

REFERENCES

1. M. Horowitz, Y. Barad, and Y. Silberberg, "Noise like pulses with a broadband spectrum generated from an erbium-doped fiber laser," Opt. Lett., **22**, 781 (1997).
2. Y. Jeong, L. A. V. Zuniga, S. Lee, and Y. Kwon, "On the formation of noise-like pulses in fiber ring cavity configurations," Opt. Fiber Technol. **20**, 575 (2014).
3. K. Özgören, B. Öktem, S. Yilmaz, F. Ö. Ilday, and K. Eken, "83 W, 3.1 MHz, square-shaped, 1 ns-pulsed all fiber-integrated laser for micro-machining," Opt. Express **19**, 17647 (2011).
4. A. Zaytsev, C. H. Lin, Y. J. You, C. C. Chung, C. L. Wang, and C. L. Pan, "Supercontinuum generation by noise-like pulses transmitted through normally dispersive standard single-mode fibers," Opt. Express **21**, 16056 (2013).
5. S. Keren and M. Horowitz, "Interrogation of fiber gratings by use of low-coherence spectral interferometry of noise like pulses," Opt. Lett. **26**, 328 (2001).
6. A. F. J. Runge, C. Aguergaray, N. G. R. Broderick, and M. Erkintalo, "Coherence and shot-to-shot spectral fluctuations in noise-like ultrafast fiber lasers,"Opt. Lett., **28**, 4327 (2013).
7. Y. Jeong, L. Alonso, V. Zuniga, S. Lee, and Y. Kwon, "Phase coherence characteristics of noise-like pulses in fiber ring cavity configurations," Opto-Electronics and Communications Conference (OECC), 1 (2015).
8. Y. Kwon, L. A. Vazquez-Zuniga, S. Lee, H. Kim, and Y. Jeong, "Numerical study on multi-pulse dynamics and shot-to-shot coherence property in quasi-mode-locked regimes of a highly-pumped anomalous dispersion fiber ring cavity,"Opt. Express **25**, 4456 (2017).
9. J. Shang, X. Lu, T. Jiang, Y. Lu, and S. Yu, "Simple and efficient nonlinear polarization evolution mode-locked fiber laser by three-dimensionally manipulating a polarization beam splitter," Opt. Lett. **43**, 3301 (2018).
10. L. E. Nelson, D. J. Jones, K. Tamura, H. A. Haus, E. P. Ippen, "Ultrashort-pulse fiber ring lasers,"Appl. Phys. B **65**, 277 (1997)
11. J. M. Dudley, S. Coen, "Coherence properties of supercontinuum spectra generated in photonic crystal and tapered optical fibers," Opt. Lett. **27**, 1180 (2002).
12. A. I. Chernykh and S. K. Turitsyn, "Soliton and collapse regimes of pulse generation in passively mode-locking laser systems," Opt. Lett. **20**, 398 (1995).
13. D. Tang, L. Zhao, and B. Zhao, "Soliton collapse and bunched noise-like pulse generation in a passively mode locked fiber ring laser," Opt. Express **13**, 2289 (2005).
14. Y. C. Tong, L. Y. Chan and H. K. Tsang, "Fibre dispersion or pulse spectrum measurement using a sampling oscilloscope," Electron. Lett. **33**, 11 (1997).
15. K. Goda, and B. Jalali, "Dispersive Fourier transformation for fast continuous single-shot measurements," Nature Photon. **7**, 102 (2012).
16. M. Liu, H. Chen, A. Luo, G. Zhou, Z. Luo, and W. Xu, "Identification of coherent and incoherent spectral sidebands in an ultrafast fiber laser," IEEE J. Sel. Top. Quantum Electron. **24**, 1100606 (2017).